

Evaluation of a mixed geometry model for the characterization of activated carbons

J.P. Toso · R.H. López · D.C.S. de Azevedo ·
C.L. Cavalcante Jr. · M.J. Prauchner ·
F. Rodríguez-Reinoso · G. Zgrablich

Received: 30 September 2010 / Accepted: 12 January 2011 / Published online: 19 January 2011
© Springer Science+Business Media, LLC 2011

Abstract The predictions of the Pure Slit Geometry Model (PSGM) and the Mixed Geometry Model (MGM) for the characterization of activated carbons (AC) are compared and tested against the behavior of the textural properties of series of AC obtained from coconut shells by varying the concentration of the chemical activation agent over a wide range. Through the analysis of results it is concluded that the MGM can be regarded as reliable as the PSGM, with an apparently more consistent description of the behavior as a function of the degree of chemical activation and superior consistency between the results for different adsorbates, like N_2 and CO_2 .

Keywords Activated carbon · Pore size distribution · Slit pores · Triangular pores

1 Introduction

Activated carbons (AC) are considered as convenient materials for a number of separation and storage processes

due to their versatility and low cost (Marsh and Rodríguez-Reinoso 2006; Rodríguez-Reinoso 2002). The development of more appropriate and efficient AC for different applications is being the subject of an important amount of research (Lee et al. 2006; Prauchner and Rodríguez-Reinoso 2008; Rios et al. 2009; Santos et al. 2010). A central problem in these developments is the determination of the Pore Size Distribution (PSD) of the material in the most accurate possible way. This problem has attracted the attention of researchers for several decades, from the early developments of Dubinin and collaborators (1975), who used the Polanyi concept of the adsorption field, up to the modern DFT (Seaton et al. 1989; Lastoskie et al. 1993; Neimark et al. 2009) and Monte Carlo simulation (Nicholson and Parsonage 1982; Molina-Sabio et al. 1994; Valladares et al. 1998; Davies et al. 1999; Vishnyakov and Neimark 2005, 2009) methods, which have the advantage that they do not assume any particular adsorption process, but rather rely on realistic gas-solid and gas-gas interactions.

A common limitation in all the above developments has always been the fact that a determined geometric shape for the pores must be assumed to represent the porous material. The structure of AC is still at the present a matter of discussion, given the complexity arising from a disordered arrangement of not well defined building blocks. Nevertheless a quite simple model has been extensively used for decades to represent such a structure, namely the Pure Slit Geometry Model (PSGM), which considers the porous material as a collection of independent slit shaped pores formed by parallel graphitic plates separated by different values of the distance S between plates, which stands for the pore size, and that a given material is characterized by a PSD (Marsh and Rodríguez-Reinoso 2006). This model has been providing satisfactory interpretation of experimental data of adsorption of gases on AC. However, as the development of

J.P. Toso · R.H. López · G. Zgrablich (✉)
Instituto de Física Aplicada (INFAP), Universidad Nacional de
San Luis-CONICET, San Luis, Argentina
e-mail: giorgio@unsl.edu.ar

D.C.S. de Azevedo · C.L. Cavalcante Jr.
Departamento de Engenharia Química, Universidade Federal do
Ceará, Fortaleza, Brazil

M.J. Prauchner
Instituto de Química, Universidade de Brasília, Brasília-DF,
Brazil

F. Rodríguez-Reinoso
Departamento de Química Inorgánica, Universidad de Alicante,
Alicante, Spain

efficient adsorption systems for gas separation and storage in the last two decades has been demanding an increasingly precise characterization of the porous material, specially in the case of the determination of the PSD for AC (Bastos Neto et al. 2007), many efforts have been devoted to develop methods to improve the determination of the PSD. Some of these methods introduce heterogeneity in the thickness of the graphitic plates (Nguyen and Bhatia 2004), in the lateral dimensions of the graphitic plates (Jagiello and Olivier 2009), in the presence of different energetic sites on the surface of the graphitic plates (Ravikovitch et al. 2000) or as geometrical rugosity of these plates (Lucena et al. 2010; Oliveira et al. 2010; Neimark et al. 2009). These improvements have been successful in eliminating spurious effects on the determination of the PSD from N_2 adsorption data due to the stepwise character of the theoretical isotherms used to fit the data.

A different approach has been proposed recently (Azevedo et al. 2009, 2010) based on the idea that pores with a different geometric shape, in addition to those with a slit shape should contribute to a better description of the porous structure. High resolution TEM images of AC improved by means of digital image processing (Fei et al. 1994; Huang et al. 2002; Rouzaud and Clinard 2002), like the one represented in Fig. 1, adapted from Huang et al. (2002), clearly show regions where an adsorbed molecule would be interacting with two graphitic plates, as in a slit pore, and smaller regions where an adsorbed molecule would be interacting with three graphitic plates simultaneously (regions indicated by arrows in the figure), which can be represented by pores with a triangular section, see Fig. 2. On the other

hand, N_2 adsorption enthalpies at very low pressure reaching 6 kcal/mol have been measured in some AC (Prasad et al. 1999; Fernández-Colinas et al. 1989; Denoyel et al. 1993; Birkett and Do 2006), which point out to an interaction of a N_2 molecule with three graphitic plates, given that the maximum adsorption energy on a single graphitic plate amounts to only about 2 kcal/mol (Azevedo et al. 2010). Based on these observations, a Mixed Geometry Model (MGM) was proposed (Azevedo et al. 2009, 2010), which represents the structure of an AC as a collection of independent slit and triangular pores of different sizes in a proportion to be determined for each sample. The MGM has already been applied to the characterization of AC obtained from coconut shells (Azevedo et al. 2010) and from peach stones (Soares Maia et al. 2010a, 2010b) with encouraging results indicating that the MGM could provide a more realistic description of the adsorption process in these materials as well as a smoothing of steps in the theoretical N_2 adsorption isotherm on the

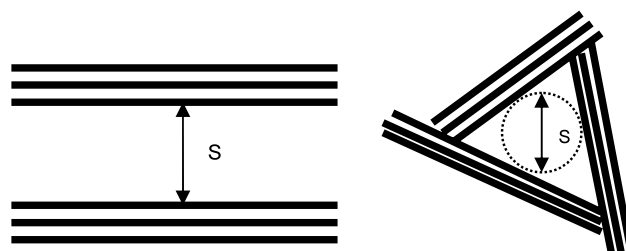


Fig. 1 Slit and triangular pores showing the distance defining the pore size S in each case

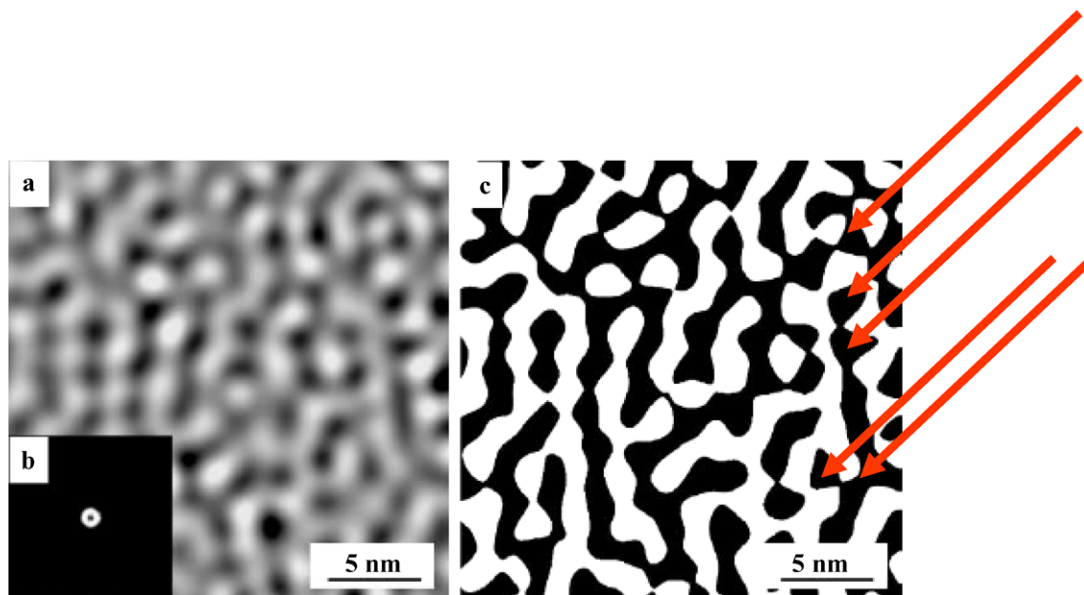


Fig. 2 High resolution TEM image, and its digitalized version, of an AC showing slit shaped pores with variable sizes and smaller regions where and adsorbing molecule would interact with 3 graphitic plates (regions marked by *arrows*) as in triangular pores. Adapted from Huang et al. (2002)

basis of the geometrical shape heterogeneity. In particular, it was found that the PSGM would systematically shift the PSD toward smaller pore sizes, due to its limitations in considering high adsorption energies at low pressure, and that the MGM seems to provide a sequence of specific surface areas for a given series of AC samples which is more consistent with the preparation method of such samples.

In the present work we intend to carry out a more rigorous test of the MGM by analyzing the adsorption of N_2 at 77 K and CO_2 at 273 K on two series of AC obtained from coconut shells by chemical activation with H_3PO_4 and $ZnCl_2$ at different P and Zn concentrations, ranging from very low to very high values (Prauchner and Rodríguez-Reinoso 2008). In Sect. 2 we briefly review the experimental and theoretical background and methodology, then results are given and discussed in Sect. 3 and, finally, conclusions are presented in Sect. 4.

2 Methodology

2.1 Experimental

We briefly describe the procedure followed by Prauchner and Rodríguez-Reinoso (2008) to obtain the AC from coconut shells used in this study. For chemical activation, the coconut shells (particle size 2.00–2.83 mm) were first impregnated with a solution of the chemical (2 mL per gram of the precursor) by stirring the mixture for 2 h at 85 °C. The solution concentration was adjusted to provide the desired ratio of phosphorous or zinc mass per gram of precursor. These ratios will be expressed from now on as X_P or X_{Zn} , respectively. At the end of the impregnation step, the solution temperature was increased to the boiling point until complete dryness. Then, the impregnated material was carbonized at 450 °C or 500 °C (for activation with H_3PO_4 and $ZnCl_2$, respectively) for 2 h (1 °C/min) under N_2 flow (100 mL/min) and subsequently washed to remove the chemical. For H_3PO_4 removal, the washing was carried out with distilled water. In the case of $ZnCl_2$, the material was first washed with a dilute solution of HCl to increase the Zn solubility and then with abundant distilled water.

Adsorption–desorption isotherms for N_2 (77 K) were determined in a Coulter Omnisorp 610 equipment in order to assess the pore morphology of the produced activated carbons. The micropore volume was calculated using the Dubinin–Radushkevich (DR) equation and the specific surface by the BET equation. In addition, CO_2 adsorption isotherms at 273 K were also measured in order to complement the AC characterization. The application of the DR equation to the CO_2 adsorption data allows the calculation of the volume of narrow micropores (up to 0.7 nm), as shown previously by Rodríguez-Reinoso et al. (1989).

2.2 Theoretical

We briefly review here the MGM developed in detail by Azevedo et al. (2010) and used to fit the experimental isotherms for both gases. Two geometries are proposed in this model to represent the idealized porous structure of an AC, the slit and triangular geometry pores; only equilateral triangles are considered for the latter in order to keep the number of parameters to a minimum and in this case the pore size is given by the diameter of the circle inscribed in the triangular section of the pore. The gas–solid potential for the slit geometry is given, as usual, by the superposition of two Steele potentials, one per each infinite plate. For the triangular geometry, the gas–solid potential is obtained by summing the contributions of three semi-infinite plates. The potential of each semi-infinite plate is given in Bojan and Steele (1998). The values of all parameters included in the interaction potentials for N_2 and CO_2 adsorption are given in Table 1.

A collection of adsorption isotherms (the local isotherms) was obtained through the GCMC simulation method in the continuum, following the algorithm outlined by Valladares et al. (1998), both for the slit and the triangular geometries. Transition probabilities for each Monte Carlo attempt, displacement, adsorption and desorption of molecules, are given by the usual Metropolis rules. Equilibrium was generally achieved after 10^7 MC attempts, after which mean values were taken over the following 10^7 MC attempts for configurations spaced by 10^4 MC attempts in order to ensure statistical independence. This collection of isotherms can be used in three ways to fit a given experimental isotherm: (a) pure slit pores; (b) pure triangular pores; (c) a mixture of slit and triangular pores, with an undetermined fraction x of slit pores.

A minimization method for the mean square error, with a regularization term, as described by Davies et al. (1999), was used to fit an experimental isotherm with the theoretical isotherm, as explained in Azevedo et al. (2010).

Table 1 Values of potential parameters for both gases

Parameter	N_2^a	CO_2^b
ε_{gs}/k_B	53.22 K	81.49 K
σ_{gs}	3.494 Å	3.429 Å
ε_{gg}/k_B	101.5 K	246.15 K
σ_{gg}	3.615 Å	3.648 Å

^aRavikovitch et al. (2000)

^bVishnyakov et al. (1999)

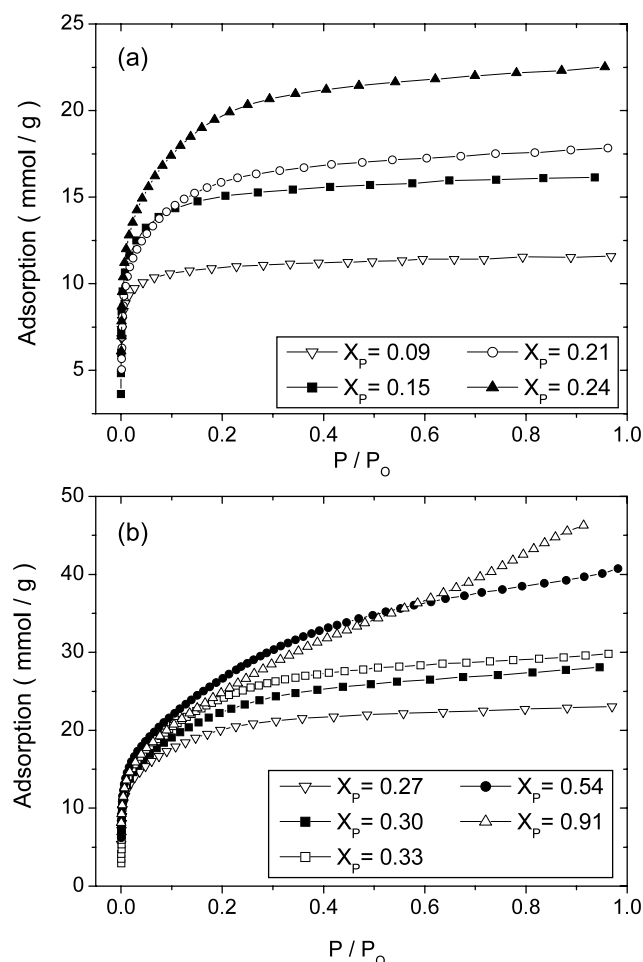


Fig. 3 Experimental adsorption isotherms for N₂ on P-samples

3 Results and discussion

Adsorption isotherms for N₂ at 77 K on samples activated with H₃PO₄, for $X_p = 0.09, 0.15, 0.21, 0.24, 0.27, 0.30, 0.33, 0.54$ and 0.91 (P-samples), are shown in Fig. 3, while those corresponding to adsorption of CO₂ at 273 K on the same samples are shown in Fig. 4. On the other hand, the adsorption isotherms for the two gases on samples activated with ZnCl₂, for $X_{Zn} = 0.15, 0.25, 0.32, 0.45, 0.50$ and 0.65 (Zn-samples), are presented in Fig. 5.

PSDs were obtained for all samples and for the two adsorbates by fitting the experimental isotherms both with the PSGM and the MGM. We only show here the PSD results for N₂ on $X_p = 0.15$ and 0.91 samples in Fig. 6, and for CO₂ in Fig. 7, and the PSDs for the same gases on $X_{Zn} = 0.15$ and 0.65 samples in Figs. 8 and 9, in such a way that the effects of the geometric shape of the pores and the adsorbate can be appreciated for low and high activation degrees.

All other textural characteristics, like BET specific surface and DR micropore volume, given by the adsorption apparatus, and the same quantities predicted by the PSGM and

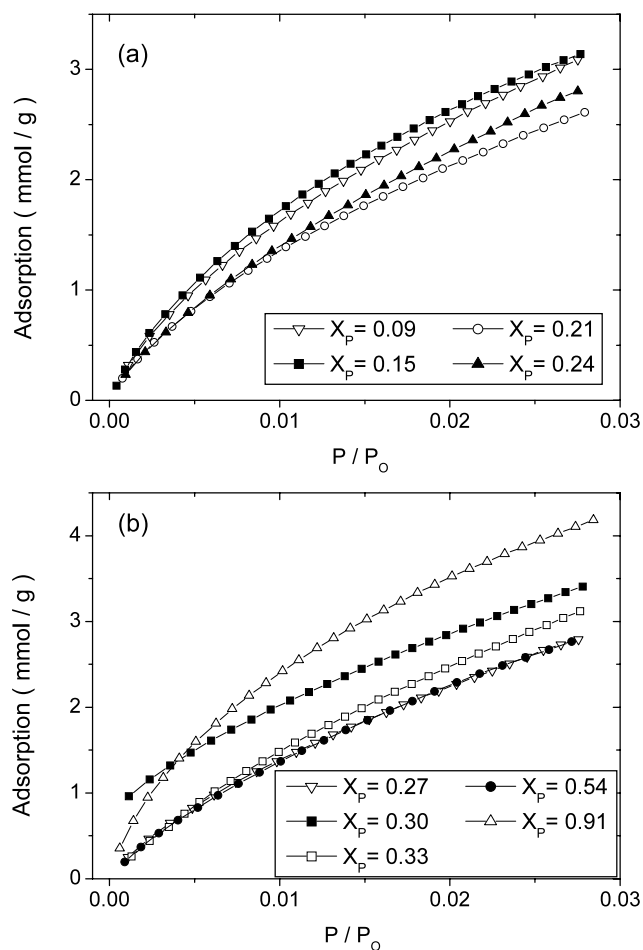


Fig. 4 Experimental adsorption isotherms for CO₂ on P-samples

the MGM, which are obtained from the PSDs, are presented in Figs. 10 to 13 for N₂ on P-samples, CO₂ on P-samples, N₂ on Zn-samples and CO₂ on Zn-samples, respectively.

In all cases both the PSGM and the MGM predicted PSDs fitted the experimental isotherms reasonably well and such fits are not shown for the sake of conciseness. By looking at Figs. 6 to 10 we can easily see that the PSGM and MGM PSDs for the same sample are always in better agreement for CO₂ adsorption than for N₂ adsorption.

We now proceed to a more detailed discussion about each of the probe gases used in each series of chemically activated samples.

3.1 N₂ on P-samples

PSGM and MGM predict in general similar trends in the behavior of the total pore volume, the volume of pores smaller than 2 nm (these are in total coincidence with the DR values) and the specific surface (here it is well known that BET over-estimates this quantity).

It is interesting to analyze in detail the behavior at low X_p (say, between 0.09 and 0.27). By looking at the behav-

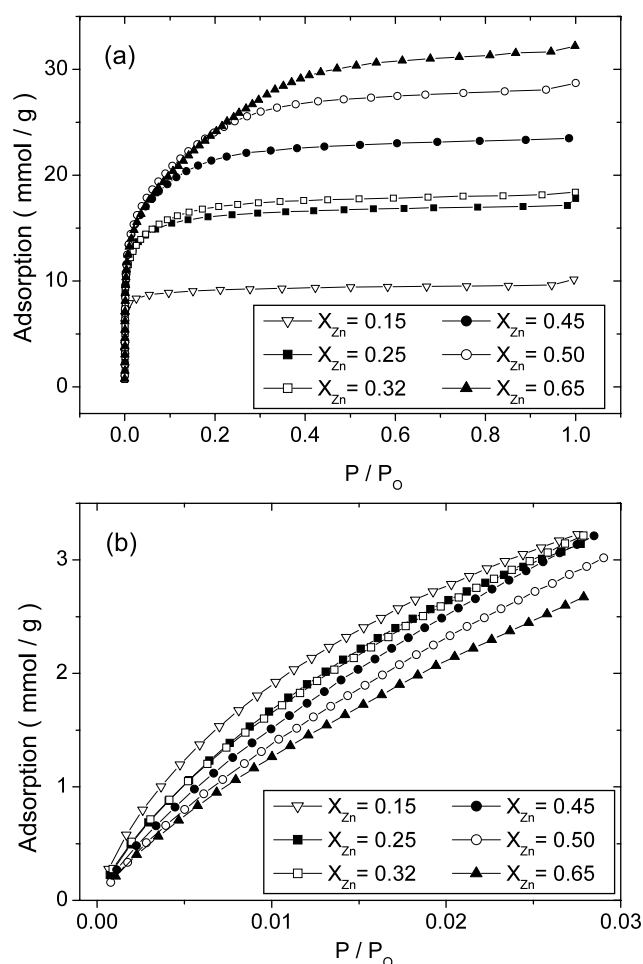


Fig. 5 Experimental adsorption isotherms for N_2 , (a), and for CO_2 , (b), on Zn-samples

ior of the volume of pores smaller than 1 nm (Fig. 10), the PSGM predicts an increase from the sample corresponding to $X_P = 0.09$ to that corresponding to $X_P = 0.15$, and therefore an appreciable increase in the specific surface, and a sudden decrease from the sample corresponding to $X_P = 0.15$ to that corresponding to $X_P = 0.21$, resulting in a sudden decrease in the specific surface. In addition, the PSGM predicts a new appearance of micropores smaller than 1 nm at $X_P = 0.30$, after having completely disappeared at $X_P = 0.21$, a fact which does not seem reasonable. This behavior is in contradiction to the predictions of the same PSGM in this region for the adsorption of CO_2 (Fig. 11, to be discussed later), in which case the behavior of the specific surface is dominated by the behavior of pores in the range from 0.8 to 1.46 nm, while those below 0.8 nm decrease steadily. This is due to the fact that the PSGM shifts the PSD toward smaller pores in order to compensate for the lack of sites where interactions of the adsorbate with 3 graphitic walls would take place (this is consistent with the appearance of an appreciable contribution of triangular pores in the PSDs for these samples). The MGM,

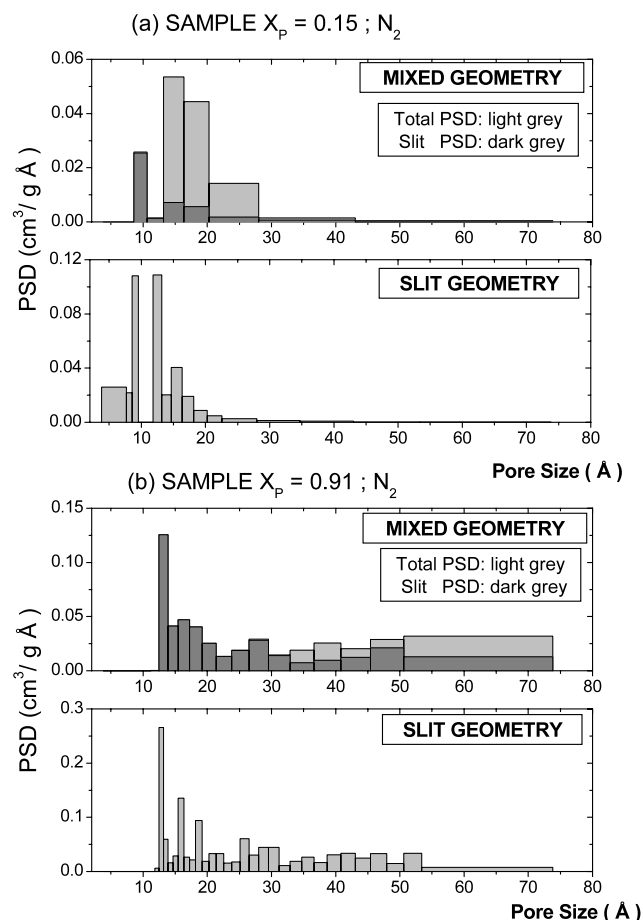


Fig. 6 PSGM and MGM PSDs for N_2 on $X_P = 0.15$, (a), and $X_P = 0.91$, (b), samples

on the contrary, predicts a smooth and monotonic decrease of the volume of pores smaller than 1 nm (in coincidence with the behavior for CO_2 adsorption in this region), which most adequately agrees with the steady increase in the activation agent concentration, and a smoother behavior of the specific surface.

In the region around $X_P = 0.30$ (Fig. 10), both the PSGM and the MGM predict a steady increase in the total pore volume, however the MGM detects a sudden decrease in the volume of pores smaller than 2 nm (also in discrepancy with the prediction of the DR equation, which assumes a pure slit geometry as well).

For the isotherm of the sample corresponding to $X_P = 0.91$ (Fig. 10), the MGM predicts a very different PSD from that corresponding to the PSGM, resulting in an increase in the pore volume of large pores in the region of mesopores and a decrease in the volume of pores smaller than 2 nm, although the specific surface is the same as that predicted by the PSGM. By looking at the isotherm (Fig. 3), we can see that its shape is in better accordance with the predictions of the MGM.

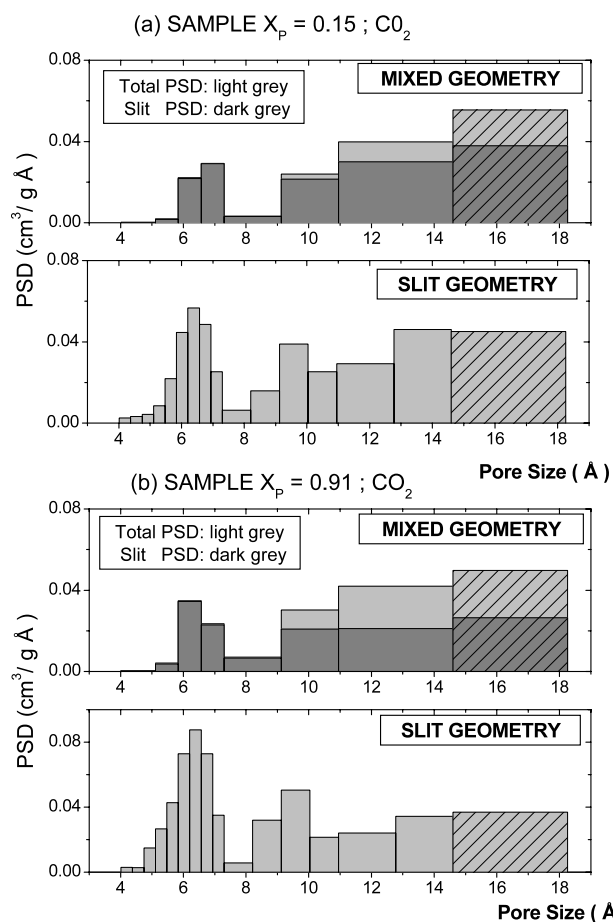


Fig. 7 PSGM and MGM PSDs for CO₂ on $X_P = 0.15$, (a), and $X_P = 0.91$, (b), samples

For all the other isotherms, the PSDs predicted by the PSGM and the MGM are in excellent agreement; moreover, the MGM predicts almost no contribution of triangular pores for those samples.

Therefore, neglecting irregularities which are probably due to unexpected changes in the sample preparation process, it is reasonable to say that the steady increase in the specific surface predicted by the MGM accounts adequately for the behavior of this parameter as X_P increases.

3.2 CO₂ on P-samples

The use of CO₂ as an adsorbate has been regarded as a convenient way of obtaining a more precise PSD in the smaller micropore region (Jagiello and Thommes 2004). In the samples used in the present study, we have found that practically all PSDs for CO₂ differ appreciably from those corresponding to N₂. This is a controversial matter, since some authors report similar PSDs for different adsorbates in the characterization of a few samples (Ravikovitch et al. 2000; Jagiello and Thommes 2004). The discrepancies can be due to several reasons: (a) The difficulty for N₂ to pen-

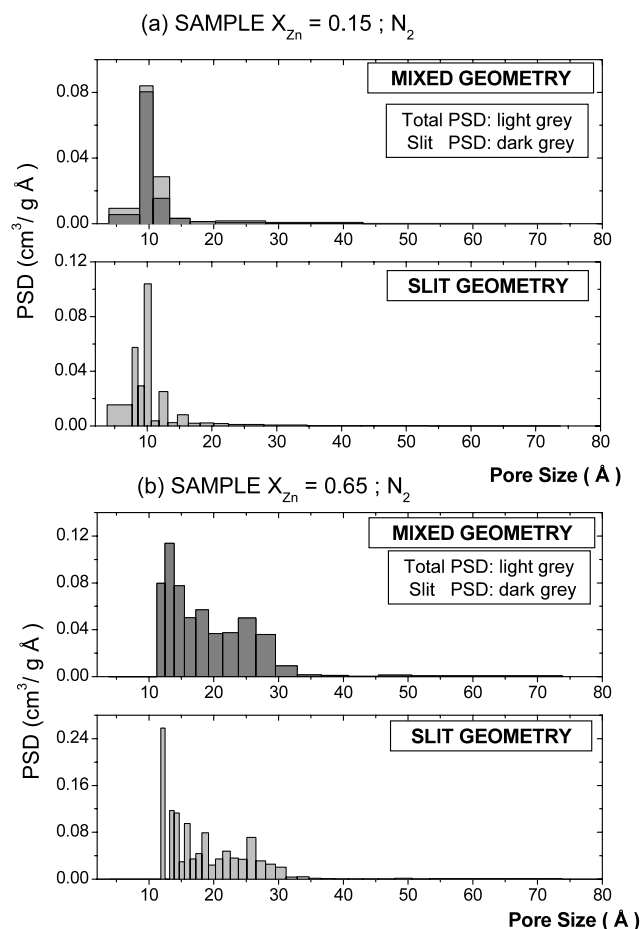


Fig. 8 PSGM and MGM PSDs for N₂ on $X_{Zn} = 0.15$, (a), and $X_{Zn} = 0.65$, (b), samples

etrate ultramicropores will produce deviations among the PSDs in the ultramicropore region; (b) The existence of a “reliability window” (Jagiello and Thommes 2004) in CO₂ isotherms, which become linearly dependent for pore sizes above 1.4 nm; (c) The fact that experimental CO₂ isotherms at 273 K are usually obtained at very low relative pressure (around 0.02) making that complete pore filling can be achieved only in small micropores (say < 1 nm) and that, in addition, CO₂ at 273 K is much closer to its bulk critical point than N₂ at 77 K, making that the filling of a pore of a given size for the former is shifted to higher relative pressures as compared to the latter, producing deviations among the PSDs in the larger micropore range. These differences among the PSDs have already been reported in Soares Maia et al. (2010b) for other ACs, but it was found that the MGM would predict more similar PSDs for both adsorbates. By comparing the PSDs obtained with N₂ and CO₂ for $X_P = 0.15$ (Figs. 6 and 7), we see that both adsorbates detect an appreciable amount of ultramicropores according to the PSGM, but the MGM does not predict these ultramicropores for N₂. We suspect that the pores detected by the PSGM in the ultramicropore region are a spurious effect

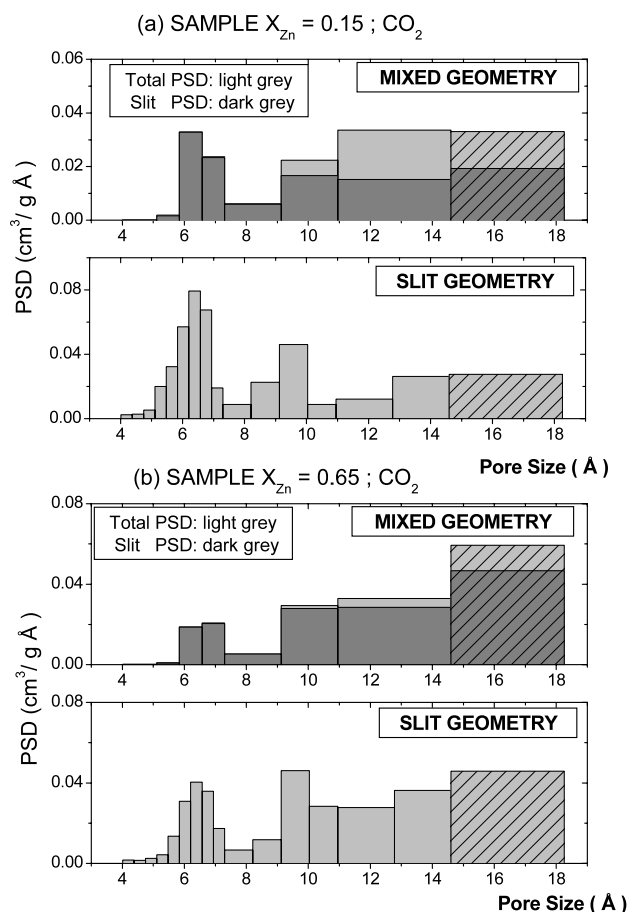


Fig. 9 PS and MG PSDs for CO_2 on $X_{\text{Zn}} = 0.15$, (a), and $X_{\text{Zn}} = 0.65$, (b), samples

due to the effort of the PS to compensate for a strong adsorption (i.e. due to the interaction with 3 graphitic plates) by considering smaller slit pores. In fact, N_2 is not likely to “see” such ultramicropores because of the kinetic difficulty in penetrating them.

Adsorption isotherms present a quite erratic behavior as a function of X_{P} . In order to correlate the models predictions with experimental results we should keep in mind the effects of the “reliability window” in the fitting procedure. For this reason the shaded area in the PSD (Figs. 7 and 9) accumulates all pores larger than 1.46 nm. Therefore, only the contribution of pores up to this size is reliable and we get an incomplete characterization.

From the pore volume and specific surface area predictions (Fig. 11), we see that both the PS and the MG account for the erratic behavior observed in the experimental isotherms, however the MG seems to represent more realistically such behavior. For example, the large increase in specific surface area predicted by the PS from $X_{\text{P}} = 0.21$ to $X_{\text{P}} = 0.24$ does not correlate well with the isotherms, which are not very different. Other characteristics in favor of the MG are: (a) specific surfaces predicted by

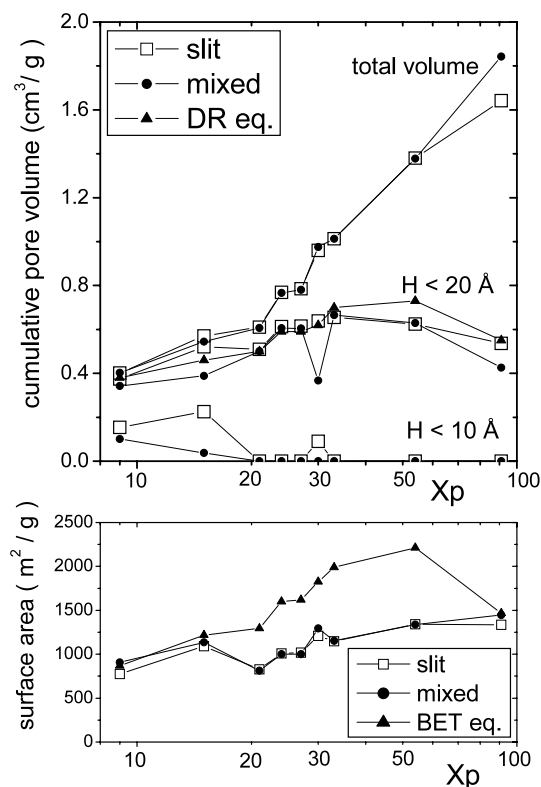


Fig. 10 Pore volume for different ranges and specific surface as a function of the concentration X_{P} for N_2 on P-samples

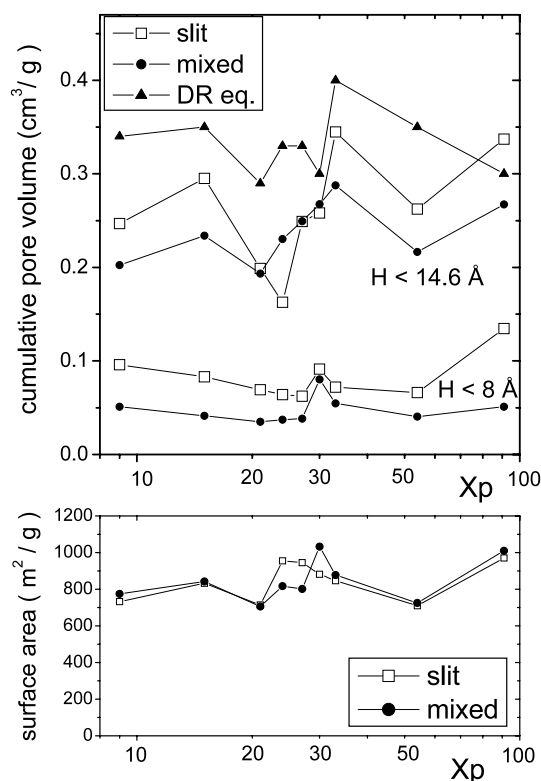


Fig. 11 Pore volume for different ranges and specific surface as a function of the concentration X_{P} for CO_2 on P-samples

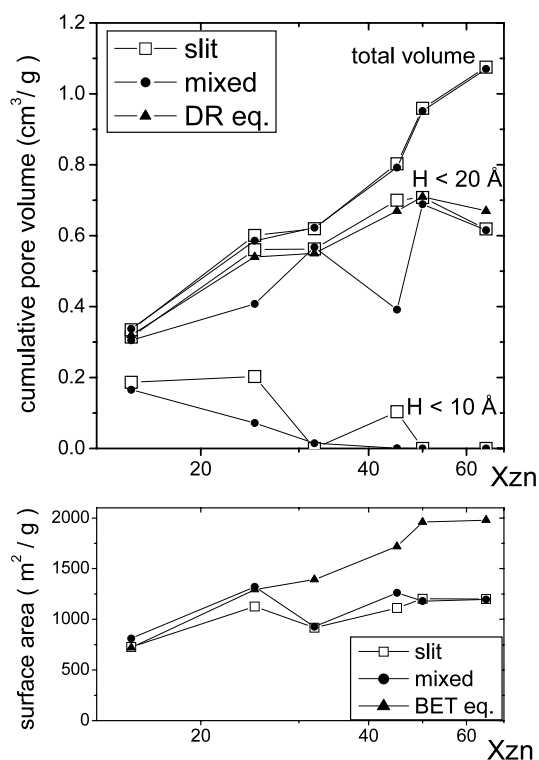


Fig. 12 Pore volume for different ranges and specific surface as a function of the concentration X_{Zn} for N_2 on Zn-samples

the MGM are almost equal for the sample corresponding to $X_P = 0.27$ and that corresponding to $X_P = 0.54$ (this is not so for the PSGM), and so are the corresponding adsorption isotherms; (b) the specific surfaces predicted by the MGM for the samples corresponding to $X_P = 0.27$, 0.30 and 0.33 follow the trend of the experimental adsorption isotherms (this is not the case for the PSGM).

In general, for CO_2 adsorption on P-samples the behavior predicted by the MGM seems to be in better conformity with the experimental data.

3.3 N_2 and CO_2 on Zn-samples

The behavior of these samples (Figs. 12 and 13) is in general more regular than that of samples activated with P. Predictions of the PSGM and the MGM are qualitatively more similar in this case. For N_2 adsorption, predicted specific surfaces are practically equal except for the samples corresponding to $X_{Zn} = 0.25$ and $X_{Zn} = 0.45$, where there is a greater contribution of triangular pores producing an appreciable difference in the specific surfaces predicted by the two models. For the adsorption of CO_2 (Fig. 13), the behavior of the predictions is similar in all cases. On the other hand, it is very difficult to explain the behavior of pores smaller than 0.8 nm predicted by the PSGM for N_2 (Fig. 12). In fact, as already noticed in analyzing Fig. 10 for P-samples, PSGM predicts that, after these smaller pores have disappeared at

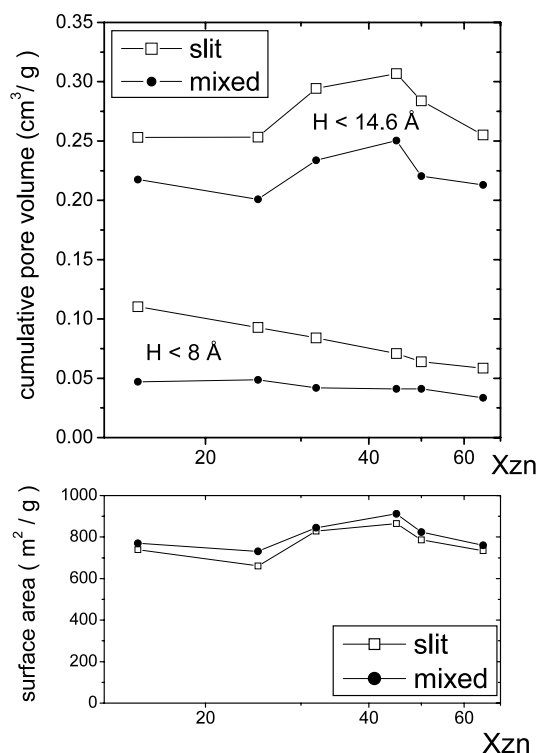


Fig. 13 Pore volume for different ranges and specific surface as a function of the concentration X_{Zn} for CO_2 on Zn-samples

$X_{Zn} = 0.32$, they again re-appear in appreciable extent at $X_{Zn} = 0.45$.

In general, we can say that the MGM provides a characterization at least as reliable as the PSGM, with an apparently more realistic description of the behavior of textural parameters as a function of the concentration of the activation agent.

4 Conclusions

The MGM for the characterization of the PSD of AC, recently proposed as an alternative to the PSGM, has been evaluated by analyzing the predictions of the textural properties of two series of AC obtained from the same precursor, coconut shells. Each of the two series was obtained by using a different activation agent, H_3PO_4 and $ZnCl_2$, respectively, and in each series only the activation agent concentration was varied. This should constitute an appropriate benchmark procedure to test characterization models.

PSDs for each sample were obtained by fitting experimental adsorption isotherms for N_2 at 77 K and CO_2 at 273 K, using Grand Canonical Monte Carlo simulated isotherms for each pore size, both considering the MGM and the PSGM. From the PSDs, other textural properties, such as the accumulated pore volume in different ranges and the specific surface, were determined.

It is important to point out that the MGM introduces only one extra-parameter (of a total of 40) as compared to the PSGM, i.e. the relative proportion of triangular to slit pores, and that both models produce good fits to experimental adsorption isotherms, therefore the evaluation of these models must be done on the basis of their ability to produce a more consistent characterization for series of activated carbons obtained through the variation of a single parameter in their synthesis processes, namely the activation agent concentration.

It was found that the predictions of the MGM and the PSGM were coincident for some samples, whereas for other samples, the MGM appears to offer a more reasonable description of the behavior of the textural parameters as the concentration of the activation agent increases and a superior consistency between the characterizations provided by N₂ and CO₂ adsorption. Therefore, we conclude that the MGM provides a characterization at least as reliable as the PSGM, with an apparently more realistic description of the progression of textural parameters of chemically activated carbons as a function of the concentration of the activation agent.

Acknowledgements This work was partially supported by CONICET (Argentina), by PETROBRAS (Brazil) and CAPES (project CAPG/BA 035-08).

References

- Azevedo, D.C.S., Cavalcante, C.L. Jr., López, R.H., Torres, A.E.B., Toso, J.P., Zgrablich, G.: Mixed geometry characterization of activated carbons PSD. In: Kaskel, S., Llewellyn, P., Rodríguez-Reinoso, F., Seaton, N.A. (eds.) *Proceedings of the 8th International Symposium on Characterization of Porous Solids VIII*, p. 211. The Royal Society of Chemistry, Cambridge (2009), ISBN:978-1-84755-904-3
- Azevedo, D.C.S., Rios, R.B., López, R.H., Torres, A.E.B., Cavalcante, C.L. Jr., Toso, J.P., Zgrablich, G.: Characterization of PSD of activated carbons by using slit and triangular pore geometries. *Appl. Surf. Sci.* **256**, 5191–5197 (2010)
- Bastos Neto, M., Canabrava, D.V., Torres, A.E.B., Rodríguez-Castellón, E., Jiménez-López, A., Azevedo, D.C.S., Cavalcante, C.L. Jr.: Effects of textural and surface characteristics of microporous activated carbons on the methane adsorption capacity at high pressures. *Appl. Surf. Sci.* **253**, 5721–5725 (2007)
- Birkett, G.R., Do, D.D.: Correct procedures for the calculation of heats of adsorption for heterogeneous adsorbents from molecular simulation. *Langmuir* **22**, 9976–9981 (2006)
- Bojan, M.J., Steele, W.A.: Computer simulation in pores with rectangular cross-sections. *Carbon* **36**, 1417–1423 (1998)
- Davies, G.M., Seaton, N.A., Vassiliadis, V.S.: Calculation of pore size distribution of activated carbons from adsorption isotherms. *Langmuir* **15**, 8235–8245 (1999)
- Denoyel, R., Fernández-Colinas, J., Grillet, Y., Rouquerol, J.: Assessment of the surface area and microporosity of activated charcoals from immersion calorimetry and nitrogen adsorption data. *Langmuir* **9**, 515–518 (1993)
- Dubinin, M.M.: In: Danielli, J.F., Rosenberg, M.D., Cadenhead, D. (eds.) *Progress in Surface and Membrane Science*, vol. 9, pp. 1–70. Academic Press, New York (1975)
- Fei, Y.Q., Yamada, Y., Meada, T., Shiraishi, M., Derbyshire, F.: High resolution TEM/digital image analysis of activated mesophases microbeads. In: *Proc. CARBON'94 Conference*, p. 202. Granada (1994)
- Fernández-Colinas, J., Denoyel, R., Grillet, Y., Rouquerol, F., Rouquerol, J.: Significance of N₂ and Ar adsorption data for following the pore structure modifications of a charcoal during activation. *Langmuir* **5**, 1205–1210 (1989)
- Huang, Z.H., Kang, F., Huang, W.L., Yang, J.B., Liang, K.M., Cui, M.L., Cheng, Z.: Pore structure and fractal characteristics of activated carbon fibers characterized by using HRTEM. *J. Colloid Interface Sci.* **249**, 453 (2002)
- Jagiello, J., Thommes, M.: Comparison of DFT characterization methods based on N₂, Ar, CO₂, and H₂ adsorption applied to carbons with various pore size distributions. *Carbon* **42**, 1225–1229 (2004)
- Jagiello, J., Olivier, J.P.: A simple two-dimensional NLDFT model of gas adsorption in finite carbon pores. Application to pore structure analysis. *J. Phys. Chem. C* **113**, 19382–19385 (2009)
- Lastoskie, C., Gubbins, K.E., Quirk, N.: Pore size distribution analysis of microporous carbons: A density functional theory approach. *J. Phys. Chem.* **97**, 4786–4796 (1993)
- Lee, J., Kim, J., Hyeon, T.: Recent progress in the synthesis of porous carbon materials. *Adv. Mater.* **18**, 2073–2094 (2006)
- Lucena, S.M.P., Paiva, C.A.S., Silvino, P.F.G., Azevedo, D.C.S., Cavalcante, C.L. Jr.: The effect of heterogeneity in the randomly etched graphite model for carbon pore size characterization. *Carbon* **48**, 2554–2565 (2010)
- Marsh, H., Rodríguez-Reinoso, F.: *Activated Carbon*. Elsevier, London (2006)
- Molina-Sabio, M., Rodríguez-Reinoso, F., Valladares, D., Zgrablich, G.: In: Rouquerol, J., Rodríguez-Reinoso, F., Sing, K.S.W., Unger, K.K. (eds.) *Characterization of Porous Solids III, Studies in Surface Science and Catalysis*, vol. 87, p. 573. Elsevier, Amsterdam (1994)
- Neimark, A.V., Lin, Y., Ravikovitch, P.I., Thommes, M.: Quenched solid density functional theory and pore size analysis of microporous carbons. *Carbon* **47**, 1617–1728 (2009)
- Neimark, A.V., Vishnyakov, A.: A simulation method for the calculation of chemical potentials in small, inhomogeneous, and dense systems. *J. Chem. Phys.* **122**, 234108 (2005)
- Nguyen, T.X., Bhatia, S.K.: Probing the pore wall structure of nanoporous carbons using adsorption. *Langmuir* **20**, 3532–3535 (2004)
- Nicholson, D., Parsonage, N.G.: *Computer Simulation and Statistical Mechanics of Adsorption*. Academic Press, London (1982)
- Oliveira, J.C.A., López, R.H., Toso, J.P., Lucena, S.M.P., Cavalcante, C.L. Jr., Zgrablich, G.: On the influence of heterogeneity of graphite plates in the determination of the pore size distribution of activated carbons. *Adsorption* (2010, in press)
- Prasad, M., Akkamaradi, B.S., Rastogi, S.C., Rhao, R.R., Srinivasan, K.: Heats of adsorption for charcoal nitrogen systems. *Carbon* **37**, 1641–1642 (1999)
- Prauchner, M.J., Rodríguez-Reinoso, F.: Preparation of granular activated carbon for adsorption of natural gas. *Microporous Mesoporous Mater.* **109**, 581–584 (2008)
- Ravikovitch, P.I., Vishnyakov, A., Russo, R., Neimark, A.V.: Unified approach to pore size characterization of microporous carbonaceous materials from N₂, Ar, and CO₂ adsorption isotherms. *Langmuir* **16**, 2311–2320 (2000)
- Rios, R.B., Silva, F.W.M., Torres, A.E.B., Azevedo, D.C.S., Cavalcante, C.L. Jr.: Adsorption of methane in activated carbons obtained from coconut shells using H₃PO₄ chemical activation. *Adsorption* **15**, 271–277 (2009)
- Rodríguez-Reinoso, F., Garrido, J., Martín-Martínez, J.M., Molina-Sabio, M., Torregrosa, R.: The combined use of different ap-

- proaches in the characterization of microporous carbons. *Carbon* **27**, 23–32 (1989)
- Rodríguez-Reinoso, F.: Production and applications of activated carbons. In: Schüth, F., Sing, K.S.W., Weitkamp, J. (eds.) *Handbook of Porous Solids*, pp. 1766–1827. Wiley/VCH, Weinheim (2002)
- Rouzaud, J.N., Clinard, C.: Quantitative high-resolution transmission electron microscopy: a promising tool for carbon materials characterization. *Fuel Process. Technol.* **77–78**, 229–235 (2002)
- Santos, C., Andrade, M., Vieira, A.L., Martins, A., Pires, J., Freire, C., Carvalho, A.P.: Templated synthesis of carbon materials mediated by porous clay heterostructures. *Carbon* **48**, 4049–4056 (2010)
- Seaton, N.A., Walton, J.P.R.B., Quirke, N.: A new analysis method for the determination of the pore size distribution of porous carbons from nitrogen adsorption measurements. *Carbon* **27**, 853–861 (1989)
- Soares Maia, D.A., Sapag, K., Toso, J.P., López, R.H., Azevedo, D.C.S., Cavalcante, C.L. Jr., Zgrablich, G.: Characterization of activated carbon from peach stones through the mixed geometry model. *Microporous Mesoporous Mater.* **134**, 181–188 (2010a)
- Soares Maia, D.A., Oliveira, J.C.A., Toso, J.P., Sapag, K., López, R.H., Azevedo, D.C.S., Cavalcante, C.L. Jr., Zgrablich, G.: Characterization of the PSD of activated carbons from peach stones for separation of combustion gas mixtures. *Adsorption* (2010b, submitted)
- Valladares, D.L., Rodríguez-Reinoso, F., Zgrablich, G.: Characterization of active carbons: the influence of the method in the determination of the pore size distribution. *Carbon* **36**, 1491–1499 (1998)
- Vishnyakov, A., Ravikovitch, P.I., Neimark, A.V.: Molecular level models for CO₂ adsorption in nanopores. *Langmuir* **15**, 8736–8742 (1999)
- Vishnyakov, A., Neimark, A.V.: Multicomponent gauge cell method. *J. Chem. Phys.* **130**, 224103 (2009)